MicroRNA-337-3p impedes breast cancer progression by targeting cyclin-dependent kinase 1

SHUXIN KONG[1], JIANYANG LIU[2], BIN ZHANG[1], FENG LV[1], YANG YU[1] and TAO QIN[3]

[1]Department of Breast Surgery, The People's Hospital of Zhengzhou University, Henan Provincial People's Hospital, Zhengzhou, Henan 450003; [2]Department of Aortic Surgery, Fuwai Central China Cardiovascular Hospital, Heart Center of Henan Provincial People's Hospital, Zhengzhou, Henan 450001; [3]Department of Hepatobiliary and Pancreatic Surgery, The People's Hospital of Zhengzhou University, Henan Provincial People's Hospital, Zhengzhou, Henan 450003, P.R. China

Received May 19, 2021; Accepted August 19, 2021

DOI: 10.3892/ol.2021.13133

Abstract. MicroRNAs (miRNAs/miRs) function as key regulators in breast cancer (BC). The present study aimed to verify the function and molecular regulation of miR-337-3p in BC cells. Bioinformatics analysis was performed to screen key genes and miRNAs associated with BC. Reverse transcription-quantitative PCR and western blot analyses were performed to detect RNA and protein expression levels. Cell Counting Kit-8, BrdU and cell adhesion assays, and flow cytometric analysis were performed to assess the biological behaviors of BC cells. The dual-luciferase reporter, RNA pull-down assays, and Pearson's correlation analysis were performed to determine the association between miRNAs and mRNAs. Bioinformatics analysis revealed that miR-337-3p and cyclin-dependent kinase 1 (CDK1) acted as key regulators in BC. In addition, miR-337-3p was expressed at low levels in BC cells and tissues, which suppressed BC progression. CDK1 expression was upregulated in BC cells and tissues, which was associated with increased cell proliferation and adhesion, as well as decreased apoptosis in BC. Notably, miR-337-3p targeted CDK1 to inhibit BC cell progression. Taken together, the results of the present study suggest that miR-337-3p plays a tumor-suppressive role in BC by targeting CDK1.

Introduction

Breast cancer (BC) is the most diagnosed cancer among women worldwide, with over one million cases and ≥400,000 females succumbing to the disease every year, accounting for 14% of total cancer deaths (1). BC is the second leading cause of cancer-associated mortality in women, following lung cancer (2). According to data published by the American Cancer Society, as of January 2019, >3,800,000 women were diagnosed with BC and >150,000 of them are living with metastatic disease that severely affects their quality of life (2). It is estimated that 12.8% of women have a high risk of developing invasive BC in their lifetime, and the mortality rate is >88.8/100,000 cases (2). Thus, it is important to identify effective novel therapeutic targets for BC.

MicroRNAs (miRNAs/miRs) function as key regulators in modulating cell proliferation, invasion, migration and apoptosis in BC (3-5). miR-337-3p, a member of the miRNA family, acts as a tumor suppressor in cancer progression. For example, overexpression of miR-337-3p decreases cell proliferation and invasion in clear cell renal cell carcinoma (6). Furthermore, miR-337-3p inhibits the growth of hepatocellular carcinoma (7) and cervical cancer (8). In BC, miR-337-3p inhibits epithelial-to-mesenchymal transition (EMT) under chronic stress by targeting STAT3 (9). However, the complexity of BC progression suggests that the regulatory mechanism on BC progression may involve multiple genes downstream of miR-337-3p. Thus, the regulatory mechanism of miR-337-3p in BC cells requires further investigation.

The cyclin-dependent kinase 1 (CDK1) gene consists of nine exons and is located on chromosome 10q21.2. CDK1 protein is a member of the Ser/Thr protein kinase family (10). Previous studies have reported that CDK1 acts as an oncogene in lung cancer (11), pancreatic ductal adenocarcinoma (12), colorectal cancer (13), bladder cancer (14) and epithelial ovarian cancer (15). In BC, CDK1 inhibition has been associated with favorable treatment outcome, suggesting that CDK1 may be a target for BC therapy (16). However, the upstream regulators of CDK1 in BC remain unknown.

The present study aimed to investigate the molecular regulation of miR-337-3p/CDK1 and further verify its role in BC. Based on a previous study (9), it was hypothesized that miR-337-3p binds to 3'-untranslated region (UTR) of CDK1 to decease its expression and inhibit BC progression.

Materials and methods

Bioinformatics analysis. GSE139038 (https://www.ncbi.nlm.nih.gov/geo/query/acc.cgi?acc=GSE139038), an mRNA

Correspondence to: Dr Tao Qin, Department of Hepatobiliary and Pancreatic Surgery, The People's Hospital of Zhengzhou University, Henan Provincial People's Hospital, 7 Weiwu Road, Jinshui, Zhengzhou, Henan 450003, P.R. China
E-mail: taoqin173@163.com

Key words: microRNA-337-3p, cyclin-dependent kinase 1, breast cancer

microarray dataset of BC and normal samples was downloaded from the Gene Expression Omnibus (GEO) database (17) (https://www.ncbi.nlm.nih.gov/geo/) that stores gene expression profiles. Genes upregulated in BC samples were screened out based on the cut-off criteria of an adjusted P<0.05 (adj.P) and $\log_2$ fold-change ($\log_2$FC) >2. The upregulated genes were uploaded to Search Tool for the Retrieval of Interacting Genes/Proteins (STRING) (18) (https://string-db.org) for Gene Ontology (GO) enrichment analysis, and the key genes were further screened. The expression patterns of the key genes in breast invasive carcinoma (BRCA) were analyzed according to The Cancer Genome Atlas (TCGA) data (19). Kaplan-Meier Plotter (20) (http://kmplot.com/analysis) or StarBase (http://starbase.sysu.edu.cn/index.php) were used to analyze the association between prognosis and the key genes and miRNAs in BC. GSE143564 (21), a miRNA microarray dataset of BC and normal samples was also downloaded from the GEO database. Based on the cut-off criteria P<0.05, and $\log_2$FC<-1, miRNAs downregulated in BC samples were screened out. TargetScan (22) was used to predict miRNA target genes. The key miRNAs were identified by overlapping the downregulated miRNAs identified in the GSE143564 dataset and TargetScan.

Clinical samples. A total of 45 paired BC and adjacent normal tissues (>3 cm from the tumor) were collected from patients (median age, 50 years; range 38-67 years) who were diagnosed with BC and underwent mastectomy at the People's Hospital of Zhengzhou University (Zhengzhou, China) between February 2019 and June 2020. The inclusion criteria were as follows: i) Pathological confirmation of BC; ii) normal cognition and no communication problems; and iii) no radiotherapy or chemotherapy prior to surgery. Exclusion criteria included: i) Patients with other breast diseases; ii) patients with other malignances; iii) serious heart, lung, kidney and other organ complex diseases; iv) patients with serious infectious diseases; and v) patients who refused to provide experimental specimens. The specimens were preserved in liquid nitrogen at -80˚C until subsequent experimentation. The present study was approved by the Ethics Committee of the People's Hospital of Zhengzhou University (approval no. 2019-10), and performed in accordance with the Declaration of Helsinki. Written informed consent was provided by all patients prior to the study start. The clinical characteristics of all patients are presented in Table I.

Cell culture. The BC cell lines, T-47D, MCF7, MDA-MB-231, SK-BR-3 and BT-474, and human normal mammary cells (MCF10A) were purchased from the American Type Culture Collection (ATCC). T-47D cells was maintained in RPMI-1640 (cat. no. 30-2001; ATCC) supplemented with 0.2 U/ml bovine insulin and 10% fetal bovine serum (FBS) (Gibco; Thermo Fisher Scientific, Inc.). MCF7 and MDA-MB-231 cells were maintained in DMEM (Gibco; Thermo Fisher Scientific, Inc.) supplemented with 10% FBS. SK-BR-3 cells were maintained in McCoy's 5A medium (Gibco; Thermo Fisher Scientific, Inc.). BT-474 cells were maintained in ATCC Hybri-Care Medium (cat. no. 46-X) supplemented with 10% FBS. MF10A cells were maintained in RPMI-1640 supplemented with 10% FBS. All cells were cultured in an incubator at 37˚C with 5% CO_2.

Table I. Clinical characteristics of patients with breast cancer (n=45).

Characteristic	Number of patients, n	Percentage, %
Age, years		
≤50	19	42.2
>50	26	57.8
Menstrual status		
Premenopausal	24	53.3
Postmenopausal	21	46.7
ER status		
Positive	25	55.6
Negative	20	44.4
Lymph node metastasis		
Positive	16	35.6
Negative	29	64.4
TNM stage		
I	9	20.0
II	14	31.1
III	20	44.4
IV	2	4.4

ER, estrogen receptor; TNM, tumor-node-metastasis.

Ttransfection. Small interfering (si)-CDK1, miR-337-3p mimic, miR-337-3p inhibitor, and their corresponding negative controls (si-NC, mimic-NC and inhibitor-NC) were purchased from Shanghai GenePharma Co., Ltd. T-47D and MCF7 cells were transfected at the exponential growth stage. T-47D and MCF7 cells ($1x10^6$) were seeded into 6-well plates in 2 ml RPMI-1640 medium (Gibco; Thermo Fisher Scientific, Inc.) supplemented with 10% FBS and cultured for 24 h until the cells reached 70% confluence. Cells were subsequently transfected with 50 nM siRNA, mimic, or inhibitor, using Lipofectamine® 2000 reagent (Invitrogen; Thermo Fisher Scientific, Inc.) and cultured in Opti-MEM serum-free medium (Gibco; Thermo Fisher Scientific, Inc.) for 6 h at 37˚C. After removing the Opti-MEM serum-free medium, fresh medium (RPMI-1640 or DMEM) supplemented with 10% FBS was added to the cells and further incubated for 48 h at 37˚C. Transfection efficiency was analyzed via reverse transcription-quantitative (RT-q)PCR and western blot analyses 48 h post-transfection. Transfectant sequences are displayed in Table SI.

RT-qPCR. RNA was isolated from BC tissues and cells using TRIzol® reagent (Invitrogen; Thermo Fisher Scientific, Inc.). A total of 200 ng of extracted RNA was reverse transcribed into cDNA using the ReverTra Ace qPCR RT kit (Toyobo Life Science). qPCR was subsequently performed using Thunderbird® SYBR® qPCR Mix (Toyobo Life Science), according to the manufacturer's instructions. The following thermocycling conditions were used for qPCR: 95˚C for 60 sec, 40 cycles of 95˚C for 15 sec and 60˚C for 30 sec.

Table II. Primer sequences used for quantitative PCR.

Gene (accession no.)	Primer sequence (5'-3')
miR-337-3p (MIMAT0000754)	Forward: CGCTTCAGCTCCTATATGA Reverse: GCGAGCACAGAATTAATACGAC
U6 (NR_004394)	Forward: GCAAATTCGTGAAGCGTTCCATA Reverse: AACGAGACGACGACAGAC
CDK1 (NM_033379)	Forward: AAATGTGTGTAGGTCTCAC Reverse: ATGATTTAAGCCAACTCAAA
β-actin (EF095209)	Forward: AGGCACCAGGGCGTGAT Reverse: GCCCACATAGGAATCCTTCTGAC

miR, microRNA; CDK1, cyclin-dependent kinase 1.

The internal references for miR-337-3p and CDK1 were U6 and β-actin, respectively. Table II lists the primer sequences used for qPCR. The $2^{-\Delta\Delta Cq}$ method (23) was used to detect the relative expression levels of miR-337-3p and CDK1.

Western blotting. Total protein was extracted from BC cells using western and immunoprecipitation (IP) cell lysis buffers (Sangon Biotech Co., Ltd.). The BCA Protein Assay kit (Sangon Biotech Co., Ltd.) was used to quantify the protein concentration. Equal amounts of proteins (20 μg) were separated via 10% SDS-PAGE, transferred onto nitrocellulose membranes (MilliporeSigma) and blocked with Tris-buffered saline and 0.1% Tween 20 (TBST) containing 5% non-fat skimmed milk at 25˚C for 3 h. The membranes were washed with TBST followed by incubation with primary antibodies against CDK1 (1:1,000; Abcam; cat. no. ab18) and β-actin (1:2,000; Abcam; cat. no. ab8226) overnight at 4˚C. Subsequently, membranes were incubated with horseradish peroxidase-conjugated secondary antibody (1:2,000; cat. no. sc-2357; Santa Cruz Biotechnology, Inc.) for 1 h at 37˚C. β-actin was used as the normalization control. SuperSignal West Pico Chemiluminescent Substrate (Pierce; Thermo Fisher Scientific, Inc.) was used to visualize the protein bands, which were analyzed using ImageJ software (Version 1.44; National Institutes of Health).

Cell Counting Kit-8 (CCK-8) assay. The CCK-8 (Abcam; cat. no. ab228554) assay was used to assess cell viability. Cells were seeded into 96-well microtiter plates at a density of $6.0x10^3$ cells/well. Following transfection for 0, 24, 48, and 72 h, 10 μl of CCK-8 solution was added to each well. Following incubation for 2 h, the absorbance was measured at a wavelength of 450 nm, using a spectrophotometric microtiter plate reader (Bio-Rad Laboratories, Inc.).

BrdU cell proliferation (ELISA). The BrdU Cell Proliferation ELISA kit (Abcam; cat. no. ab126556) was used. T-47D and MCF7 cells were plated at a density of $2x10^5$ cells/ml in 100 μl/well cell culture media. Following transfection for 48 h, 20 μl of BrdU reagent was diluted twice and pipetted into the cells. The plates were centrifuged for 5 min at 300 x g, 4˚C. The media was aspirated and fixing solution (200 μl/well) was added to the cells. Following incubation at room temperature for 30 min, the fixing solution was aspirated, and the plate was washed three times with wash buffer. Cells were incubated with anti-BrdU monoclonal antibody (100 μl/well; 1:500) for 1 h at room temperature. After washing the plates, 100 μl/well peroxidase goat anti-mouse IgG conjugate (1:500) was added to the cells and incubated for 30 min at room temperature. Subsequently, 100 μl/well TMB peroxidase substrate was added to the cells and incubated for 30 min at room temperature. Finally, 100 μl of stop solution was added to each well and a spectrophotometric microtiter plate reader was used to measure the absorbance at a wavelength of 450 nm.

Cell adhesion assay. Fibronectin (Sigma-Aldrich; Merck KGaA) was used to coat 96-well plates overnight, and the plates were subsequently blocked with 1% BSA (Sigma-Aldrich; Merck KGaA) at 37˚C for 2 h. Cells ($3x10^4$) were seeded into 96-well plates with serum-free RPMI-1640 medium (ATCC). Following incubation for 1 h, the non-adherent cells were washed and 10 μl/well MTT substrate was added to the adherent cells and incubated for an additional 2 h. Then, 150 μl acidic isopropanol (0.1 N HCL and isopropanol) was added to dissolve the purple formazan crystals, and the plates were kept in the dark at room temperature for 15 min. Then, 100 μl supernatant solution from each sample was transferred into a 96-well plate. Absorbance was measured at a wavelength of 570 nm, using a spectrophotometric microtiter plate reader.

Flow cytometric analysis. The Annexin V-FITC Apoptosis Detection kit (cat. no. BMS500FI-100; Invitrogen; Thermo Fisher Scientific, Inc.) was used in the present study. T-47D and MCF7 cells were trypsinized after 48 h of transfection and resuspended in 200 μl of 1X binding buffer at a cell density of $5x10^5$ cells/ml. Subsequently, Annexin V-FITC (5 μl) and 10 μl propidium iodide (PI) was added to the cells and incubated for 10 min at room temperature. Cell apoptosis was detected using FACS (BD Biosciences) and CellQuest software (version 5.1; Becton, Dickinson and Company) was used to analyze the results.

Wound healing assay. Following transfection, $1x10^5$ cells were seeded into 6-well plates and cultured until they reached 90% confluence. Subsequently, a 200-μl sterile pipette was used to scratch the cell monolayers. After removing the non-adherent cells, cells were cultured for 24 h in serum-free RPMI-1640

medium. The images of the wounds at 0 and 24 h were observed at x100 magnification under a light microscope (DM2000; Leica Microsystems, Inc).

Transwell assay. After coating the Transwell chamber with Matrigel® (Corning, Inc.), $5x10^4$ cells were added to the upper chamber in serum-free RPMI-1640 medium. Subsequently, 500 μl of medium containing 10% FBS was added to the lower chamber. Following incubation for 24 h at 37˚C, the invasive cells on the lower surface were fixed with methanol at 25˚C for 10 min and stained with 0.1% crystal violet at 25˚C for 20 min. Cells were observed at x200 magnification under a light microscope.

Dual-luciferase reporter assay. Wild-type (WT) CDK1 3'-UTR and mutant (MUT) CDK1 3'-UTR (without the binding sites) were purchased from Shanghai GenePharma Co., Ltd. The CDK1 3'-UTR WT and MUT sequences were cloned into the pGL3 basic vector (Promega Corporation) to generate pGL3-CDK1-3'-UTR WT and pGL3-CDK1-3'-UTR MUT constructs. T-47D and MCF7 cells were seeded into 6-well plates and cultured until 60-80% confluence. Cells were subsequently co-transfected with pGL3-CDK1-3'-UTR WT and pGL3-CDK1-3'-UTR MUT and miR-337-3p mimic/miR-NC, using Lipofectamine® 2000 (Invitrogen; Thermo Fisher Scientific, Inc.). After 24 h, cells were lysed, and luciferase activity was detected using the Dual-Luciferase Reporter Assay System (Promega Corporation). Relative luciferase activity normalized to *Renilla* luciferase activity.

RNA pull-down assay. Biotinylated miR-377-3p (Bio-miR-377-3p) and the corresponding NC (Thermo Fisher Scientific, Inc.) were transfected into T-47D and MCF7 cells, using Lipofectamine® 2000 reagent (Invitrogen; Thermo Fisher Scientific, Inc.). Cells were lysed with 500 μl immunoprecipitation (IP) buffer (20 mM Tris-HCl, pH 8.0, 200 mM NaCl, 1 mM EDTA, 1 mM EGTA, 0.5% Triton X-100, 0.4 U/μl RNasin, protease inhibitor cocktail) for 1 h at 4˚C, and centrifuged at 14,000 x g for 15 min at 4˚C. Then, 500 μl cell lysates were incubated with 10 μl Dynabeads M-280 Streptavidin (Invitrogen; Thermo Fisher Scientific, Inc.) according g to the manufacturer's protocol. In brief, the beads were washed 3 times using RNase-free solutions (Sigma-Aldrich; Merck KGaA) by centrifugation at 5,000 x g for 5 min (4˚C). After Bio-miR-377-3p was incubated at room temperature for 10 min on a rotator, 10 mM EDTA (pH 8.2) with 95% formamide (Sigma-Aldrich; Merck KGaA) was added to the immobilized miR-377-3p fragment at 65˚C for 5 min. The bound RNAs were isolated using TRIzol® reagent and RT-qPCR analysis was performed to detect the expression levels of the bound targets.

Statistical analysis. Statistical analysis was performed using SPSS software (version 19.0; IBM Corp.). Data are presented as the mean ± SD. Paired or unpaired Student's t-test was used to compare differences between two groups, while one-way or two-way ANOVA followed by Dunnett's or Tukey's post hoc test were used to compare differences between multiple groups. Pearson's correlation analysis was performed to analyze the correlations between miR-337-3p and CDK1 expression in BC tissues. Kaplan-Meier plotter analysis was applied to assess the relationship between gene expression and individual overall survival. Associations between miR-337-3p/CDK1 expression and clinical characteristics were analyzed by Fisher's exact test. $P<0.05$ was considered to indicate a statistically significant difference.

Results

CDK1 and miR-337-3p are key regulators in BC. Based on the cut-off criteria of adj.$P<0.05$ and $\log_2FC>2$, 64 key differentially expressed genes were identified in the GSE139038 dataset (consisting of BC samples) downloaded from the GEO database. Following STRING analysis, 11 genes were confirmed to be associated with cell proliferation (Fig. 1A). In TCGA data, CDK1 and CKS2 were upregulated in BRCA among the 11 genes (Fig. 1B). For prognosis of BC, CDK1 was closely associated with the prognosis of BC (Fig. 1C) compared with CKS2, that was not significantly associated with the prognosis of BC (Fig. S1A), according to the data from the Kaplan-Meier plotter analysis. To identify the key miRNAs in BC, downregulated miRNAs were screened from the GSE143564 dataset using the cut-off criteria of $P<0.05$ and $\log_2FC<-1$, and the miRNAs that bind to CDK1 3'-UTR were predicted using TargetScan. A total of three miRNAs (miR-548aj-3p, miR-3685 and miR-337-3p) overlapped in the GSE143564 and TargetScan (Fig. 1D) data. Among these three miRNAs, miR-337-3p was closely associated with BC prognosis (Fig. 1E), whereas miR-3685 and miR-548aj-3p were not significantly associated with BC prognosis (Fig. S1B and C). Therefore, it was hypothesized that CDK1 and miR-337-3p are key regulators in BC.

miR-337-3p suppresses BC progression. To confirm the potential role of miR-337-3p in BC, its expression was detected in BC tissues and cells. The results demonstrated that miR-337-3p was expressed at low levels in BC tissues and cells (Fig. 2A and B). miR-337-3p expression was associated with estrogen receptor (ER) status ($P=0.013$) and lymph node metastasis ($P=0.010$); however, its expression was not significantly associated with age, menstrual status or TNM stage (Table III). miR-337-3p expression decreased by >50% in T-47D and MCF7 cells compared with human normal mammary cells (MCF10A) (Fig. 2B). Thus, T-47D and MCF7 cell lines were selected for subsequent experimentation. The present study assessed the transfection efficiency of miR-337-3p mimics or inhibitor in T-47D and MCF7 cells. The results demonstrated that miR-337-3p expression increased >3-fold following transfection with miR-337-3p mimics and decreased to 70% following transfection with the miR-337-3p inhibitor compared with their respective NCs (Fig. 2C). A series of functional assays were performed to verify the proliferation, adhesion and apoptosis of T-47D and MCF7 cells. The results of the CCK-8 and BrdU assays demonstrated that BC cell viability and proliferation were inhibited following transfection with miR-337-3p mimic, and activated following transfection with the miR-337-3p inhibitor (Fig. 2D and E). Furthermore, the cell adhesion assay demonstrated that BC cell adhesion was impaired following overexpression of miR-337-3p and enhanced following miR-337-3p knockdown

Table III. Association between miR-337-3p/CDK1 expression and clinical characteristics.

	miR-337-3p expression			CDK1 expression		
Characteristic	Low (n=25)	High (n=20)	P-value	Low (n=22)	High (n=23)	P-value
Age, years			0.736			0.436
≤50	10	9		8	11	
>50	15	11		14	12	
Menstrual status			0.423			0.661
Premenopausal	12	12		11	13	
Postmenopausal	13	8		11	10	
ER status			0.013[a]			0.002[b]
Positive	18	7		7	18	
Negative	7	13		15	5	
Lymph node metastasis			0.010[b]			0.017[a]
Positive	13	3		4	12	
Negative	12	17		18	11	
TNM stage			0.100			0.115
I	2	7		6	3	
II	9	5		9	5	
III	12	8		7	13	
IV	2	0		0	2	

[a]P<0.05; [b]P<0.01. P-value was analyzed using Fisher's exact test. ER, estrogen receptor; TNM, tumor-node-metastasis.

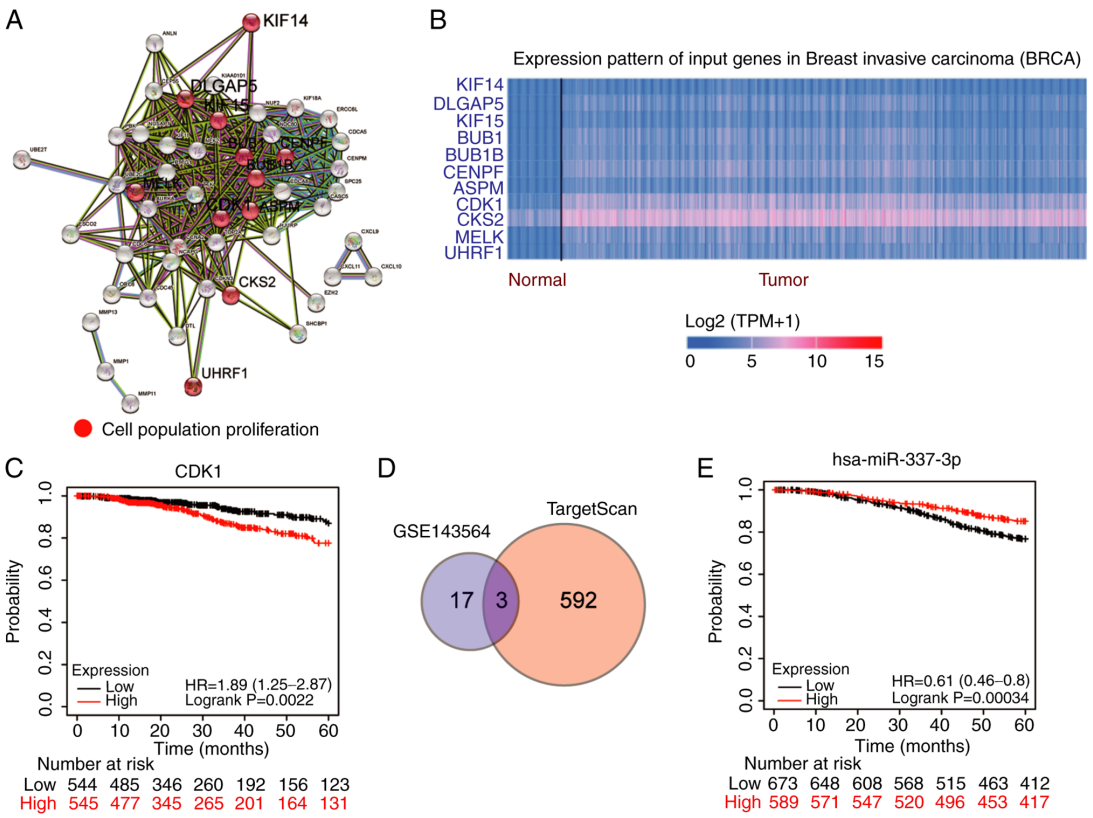

Figure 1. CDK1 and miR-337-3p are closely associated with BC. (A) Search Tool for the Retrieval of Interacting Genes/Proteins analysis identified 11 genes associated with cell proliferation. (B) CDK1 expression was significantly upregulated in breast invasive carcinoma based on The Cancer Genome Atlas database. (C) CDK1 was closely associated with the prognosis of BC. The data from Kaplan-Meier plotter with mRNA RNA-seq to overall survival. (D) Three miRNAs were overlapped from GSE143564 and TargetScan. GSE143564 included differentially expressed miRNAs in BC samples. TargetScan included the miRNAs binding to the CDK1 3'-untranslated region. (E) miR-337-3p was closely associated with the prognosis of BC. CDK1, cyclin-dependent kinase 1; miRNA/miR, microRNA; BC, breast cancer.

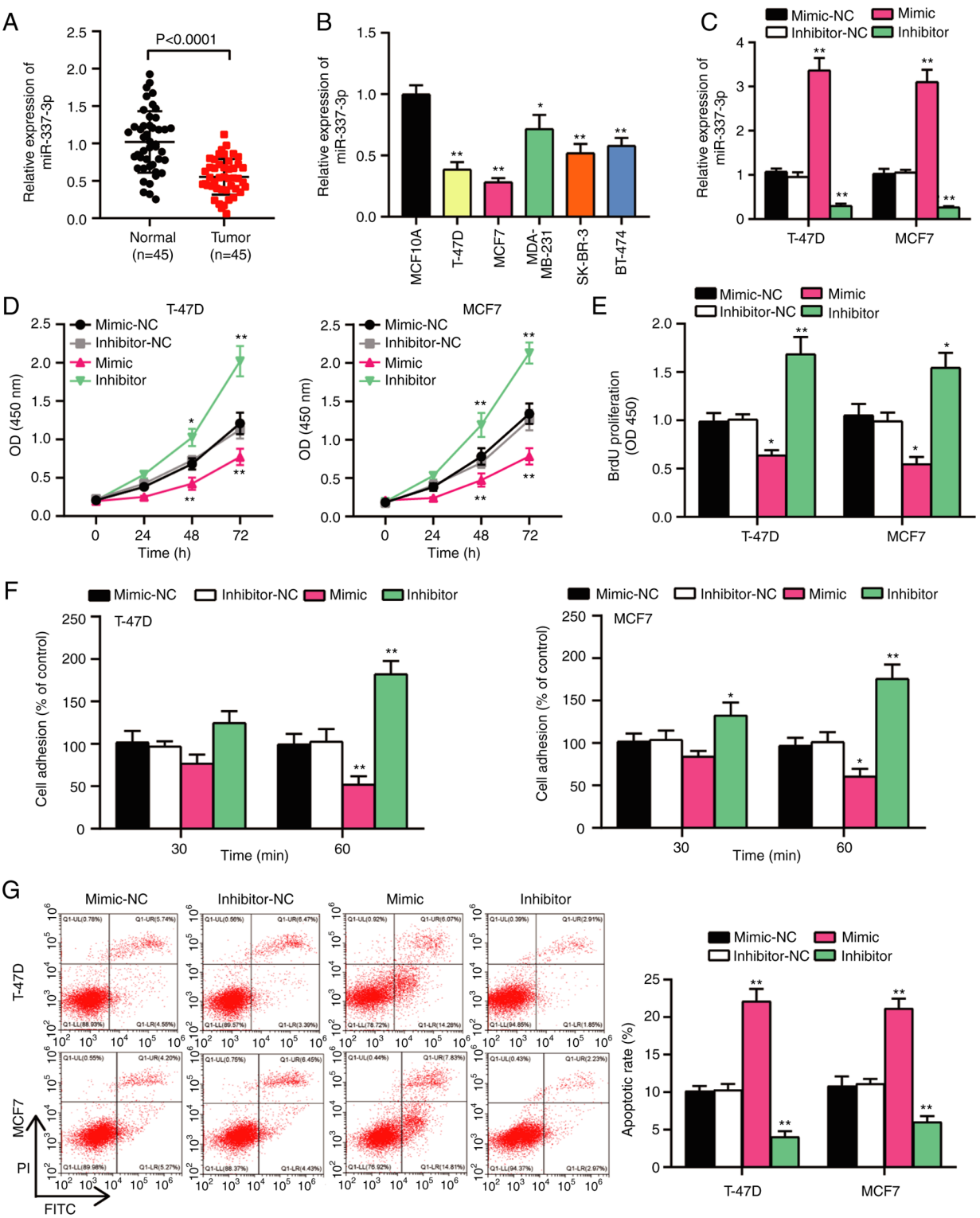

Figure 2. miR-337-3p suppresses the proliferation and adhesion but promotes the apoptosis of BC cells. (A) RT-qPCR analysis was performed to detect miR-337-3p expression in BC and normal tissues. (B) RT-qPCR analysis was performed to detect miR-337-3p expression in BC cells (T-47D, MCF7, MDA-MB-231, SK-BR-3 and BT-474) and human normal mammary cells (MCF10A). *P<0.05 and **P<0.001 vs. MCF10A cells using one-way ANOVA. (C) Overexpression and inhibition efficiency in T-47D and MCF7 cells was verified via RT-qPCR analysis. (D and E) The Cell Counting Kit-8 and BrdU assays were performed to assess the viability and proliferation of T-47D and MCF7 cells. (F) Cell adhesion of T-47D and MCF7 cells was assessed following overexpression or inhibition of miR-337-3p. (G) Flow cytometric analysis was performed to assess the apoptosis of T-47D and MCF7 cells. (C-G) *P<0.05 and **P<0.001 vs. mimic-NC or inhibitor-NC using two-way ANOVA. miR, microRNA; BC, breast cancer; RT-qPCR, reverse transcription-quantitative PCR; NC, negative control; OD, optical density.

(Fig. 2F). Flow cytometry was performed to assess cell apoptosis, and the results demonstrated that the apoptotic rate increased >2-fold following transfection with miR-337-3p mimic and decreased by almost 50% following transfection with miR-337-3p inhibitor (Fig. 2G). Furthermore, transfection with miR-337-3p mimic inhibited cell migration and invasion,

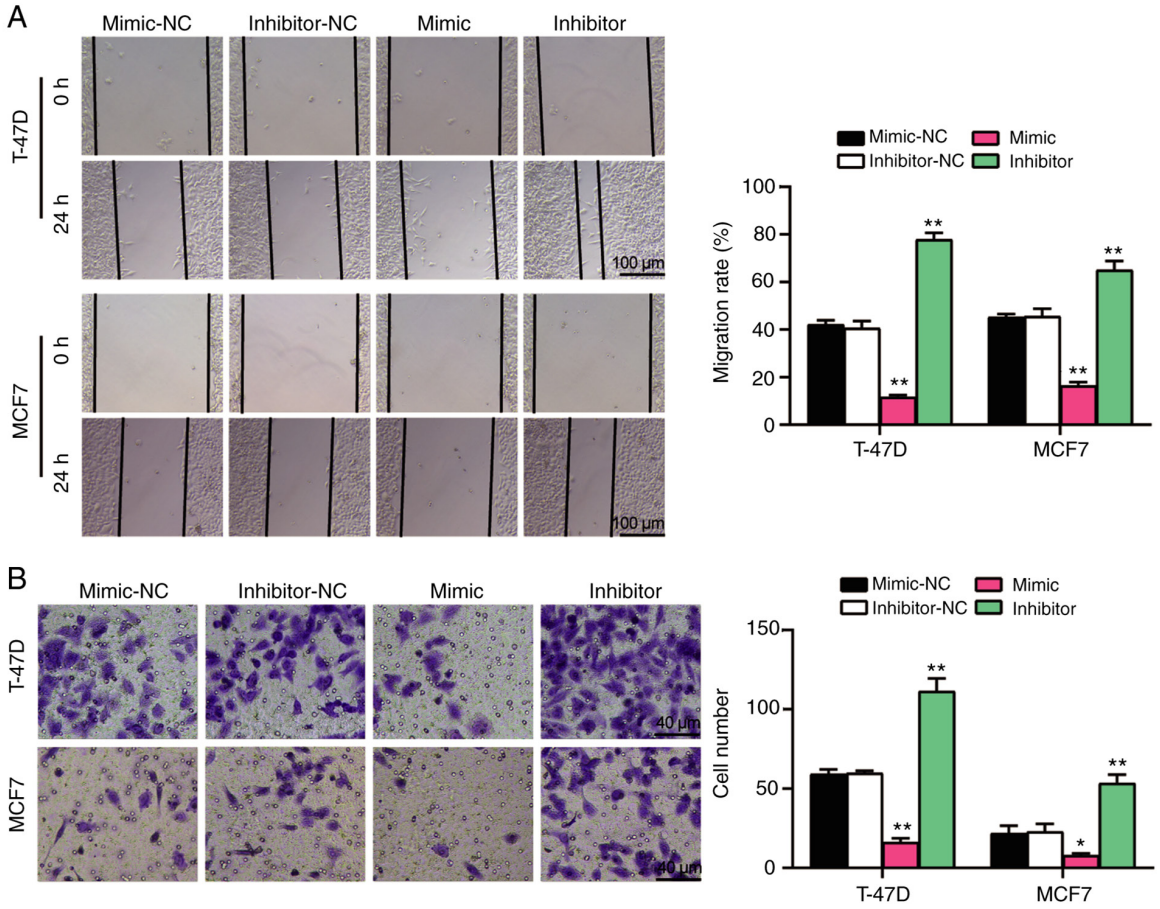

Figure 3. miR-337-3p suppresses the migration and invasion of breast cancer cells. (A) The wound healing assay was performed to assess the migratory ability of T-47D and MCF7 cells. (B) The Transwell assay was performed to assess the invasive ability of T-47D and MCF7 cells. *P<0.05, **P<0.001 vs. mimic-NC or inhibitor-NC using two-way ANOVA. miR, microRNA; NC, negative control.

whereas transfection with miR-337-3p inhibitor promoted cell migration and invasion (Fig. 3A and B). Taken together, these results suggest that miR-337-3p acts as a tumor suppressor in BC cells.

Identification of the miR-337-3p/CDK1 axis in BC cells. The present study investigated the association between miR-337-3p and CDK1 in BC cells. The TargetScan database predicted a binding site at position 544-550 of the CDK1 3'-UTR (Fig. 4A). To confirm the binding stringency of miR-337-3p and CDK1, the dual-luciferase reporter and RNA pull-down assays were performed (Fig. 4B and C). The results demonstrated that the relative luciferase activity of the CDK1 WT sequence markedly decreased by ~50% compared with the CDK1 MUT type. Similarly, CDK1 was pulled down in T-47D and MCF7 cells following transfection with bio-miR-337-3p. Furthermore, miR-337-3p inhibited CDK1 expression in both time- and dose-dependent manners (Fig. S2). CDK1 expression was detected via RT-qPCR analysis, and the results demonstrated that CDK1 was aberrantly upregulated in BC tissues (Fig. 4D). In addition, CDK1 expression was significantly associated with ER status (P=0.002) and lymph node metastasis (P=0.017) (Table III). Pearson's correlation analysis exhibited a negative correlation between miR-337-3p and CDK1 in BC cells (Fig. 4E). Western blot analysis demonstrated that CDK1 protein expression was upregulated in BC tissues (Fig. 4F). Furthermore, RT-qPCR and western blot analyses demonstrated that CDK1 expression increased in T-47D and MCF7 cells (Fig. 4G and H). Taken together, these results suggest that the miR-337-3p/CDK1 axis is involved in BC cells.

miR-337-3p/CDK1 axis modulates BC progression. To determine the changes in biological behavior of BC cells induced by the miR-337-3p/CDK1 axis, a series of rescue assays were performed. Changes in CDK1 mRNA and protein expression levels were detected following overexpression of miR-337-3p or CDK1 knockdown (Fig. 5A and B). The results demonstrated that CDK1 expression increased following miR-337-3p inhibition and reduced following CDK1 knockdown. Notably, these effects were reversed following transfection with miR-337-3p inhibitor + si-CDK1. The results of the CCK-8 and BrdU assays demonstrated that cell viability and proliferation increased and decreased, respectively, when miR-337-3p was knocked down or CDK1 was inhibited. Notably, the effects on cell proliferation were reversed following transfection with miR-337-3p inhibitor + si-CDK1 (Fig. 5C and D). Furthermore, cell adhesion increased following miR-337-3p knockdown and decreased following CDK1 knockdown, respectively. These effects were reversed following transfection with miR-337-3p inhibitor + si-CDK1 (Fig. 5E). Cell apoptosis was enhanced following CDK1 inhibition and reduced following miR-337-3p knockdown, the effects

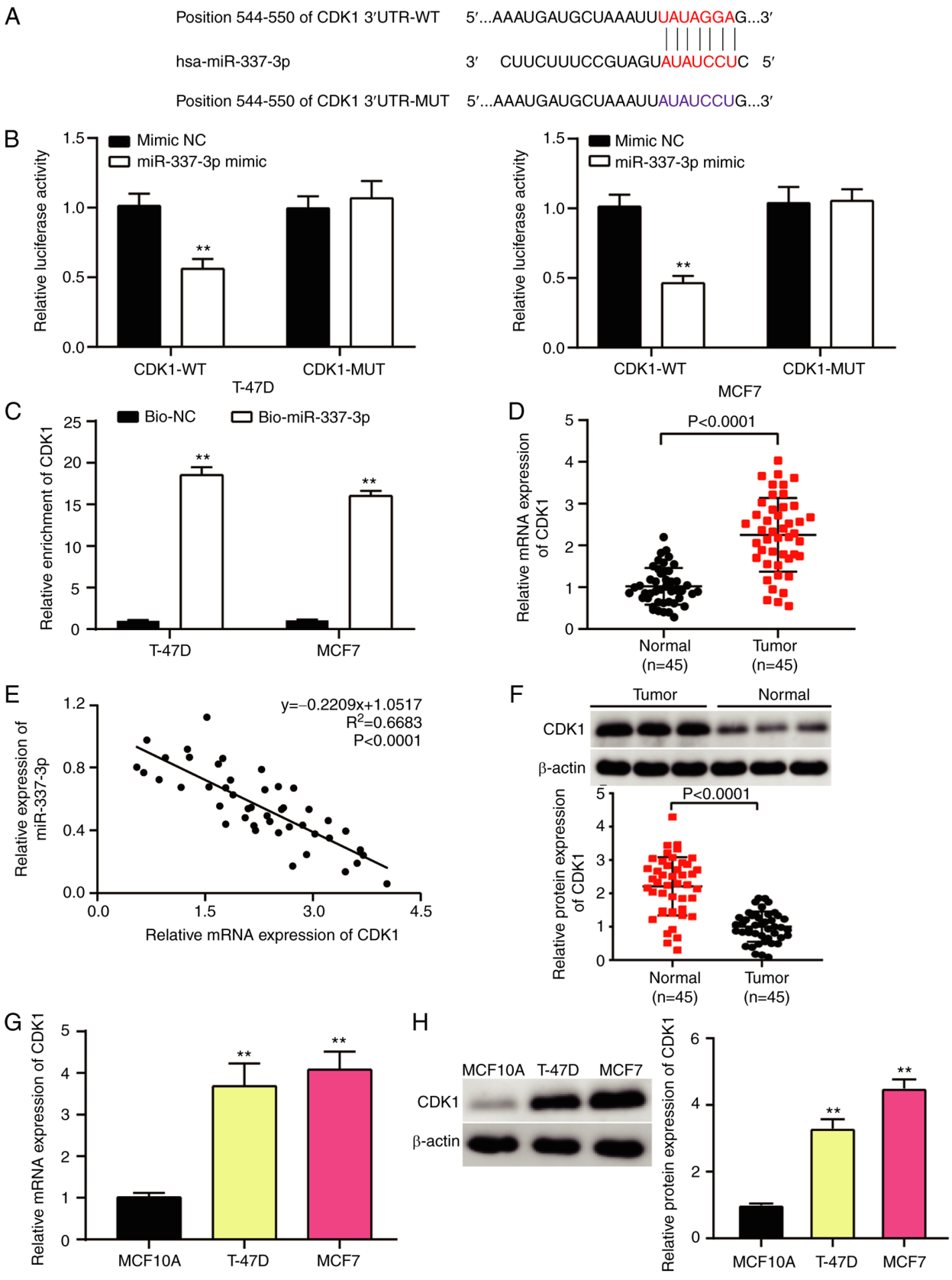

Figure 4. miR-337-3p/CDK1 axis is present in BC cells. (A) The binding site between miR-337-3p and CDK1 was identified using the TargetScan database. (B) Dual-luciferase reporter assay was performed to identify the targeting association between miR-337-3p and CDK1 in T-47D and MCF7 cells. **P<0.001 vs. mimic-NC using two-way ANOVA. (C) RNA pull down assay was performed to identify the targeting association between miR-337-3p and CDK1 in T-47D and MCF7 cells. **P<0.001 vs. Bio-NC using two-way ANOVA. (D) RT-qPCR analysis was performed to detect CDK1 expression in BC and normal tissues. (E) Pearson's correlation analysis was performed to determine the correlation between miR-337-3p and CDK1. (F) Western blot analysis was performed to detect CDK1 protein expression in BC and normal tissues. (G) RT-qPCR analysis was performed to detect CDK1 expression in MCF10A, T-47D and MCF7 cells. (H) Western blot analysis was performed to detect CDK1 protein expression in MCF10A, T-47D and MCF7 cells via. **P<0.001 vs. MCF-10A using one-way ANOVA. miR, microRNA; CDK1, cyclin-dependent kinase 1; BC, breast cancer; RT-qPCR, reverse transcription-quantitative PCR; NC, negative control; WT, wild-type; MUT, mutant.

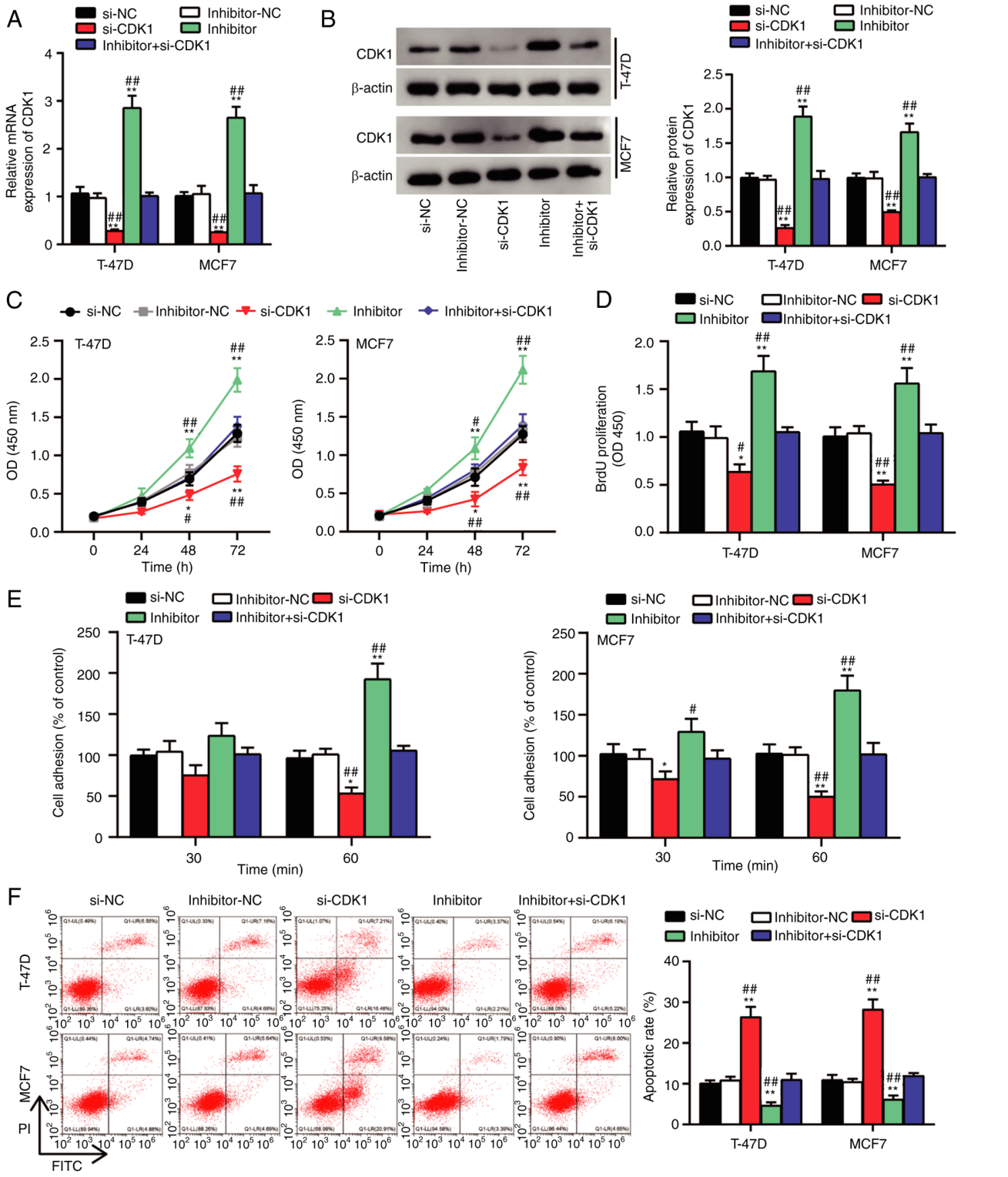

Figure 5. miR-337-3p/CDK1 axis can modulate the proliferation, adhesion and apoptosis of breast cancer cells. (A and B) Reverse transcription-quantitative PCR and western blot analyses were performed to detect the changes in expression levels of CDK1 in T-47D and MCF7 cells. (C and D) The Cell Counting Kit-8 and BrdU assays were performed to assess the viability and proliferation of T-47D and MCF7 cells. (E) Cell adhesion was assessed in T-47D and MCF7 cells. (F) Flow cytometric analysis was performed to assess the apoptosis of T-47D and MCF7 cells. *P<0.05, **P<0.001 vs. si-NC or inhibitor-NC; $^{\#}$P<0.05, $^{\#\#}$P<0.001 vs. inhibitor + si-CDK1 using two-way ANOVA. miR, microRNA; CDK1, cyclin-dependent kinase 1; si, small interfering; NC, negative control; OD, optical density.

of which were reversed following transfection with miR-337-3p inhibitor + si-CDK1 (Fig. 5F). Furthermore, cell migration and invasion were impaired following transfection with si-CDK1; however, the negative effect of si-CDK1 on cell migration and invasion was relieved following transfection with miR-337-3p inhibitor (Fig. 6A and B). Taken together, these results suggest that the miR-337-3p/CDK1 axis modulates the proliferation, adhesion and apoptosis of BC cells.

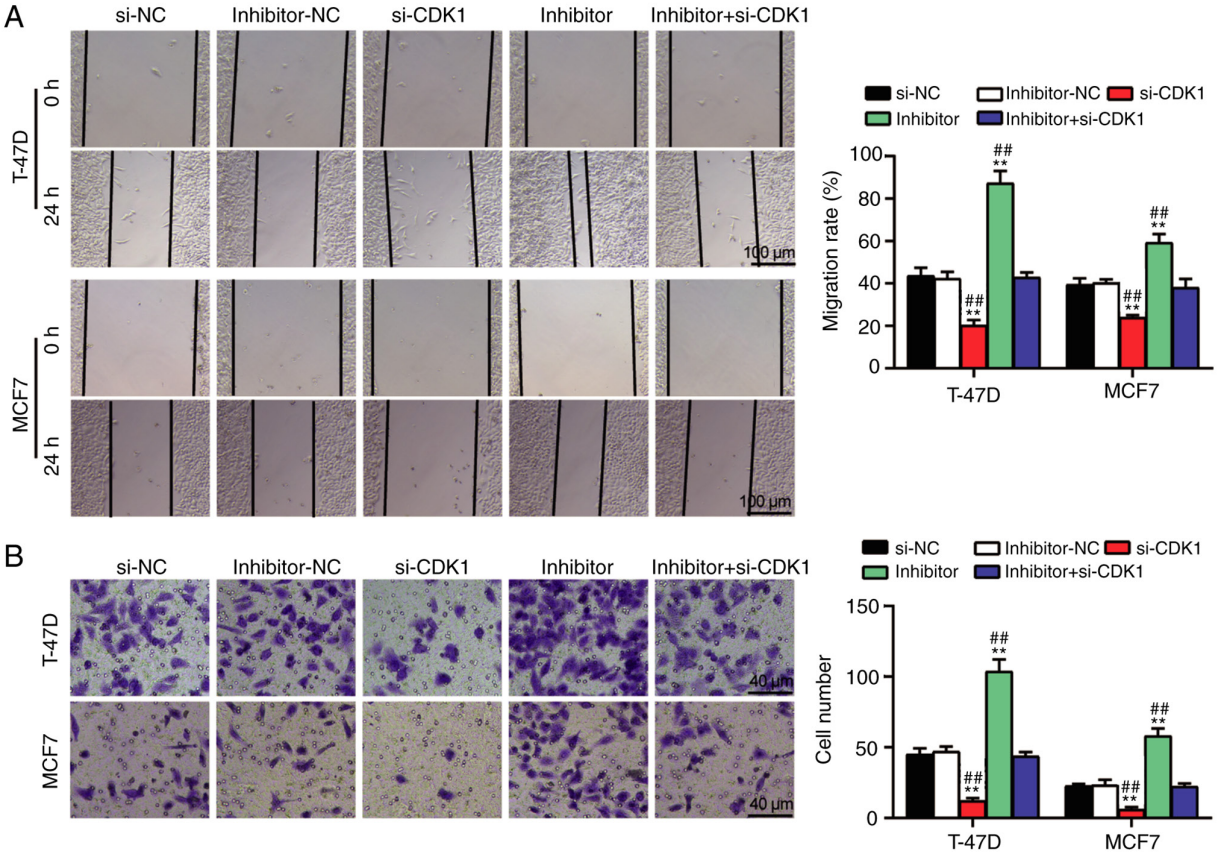

Figure 6. miR-337-3p/CDK1 axis can modulate the migration and adhesion of breast cancer cells. (A) The wound healing assay was performed to assess the migratory ability of T-47D and MCF7 cells. (B) The Transwell assay was performed to assess the invasive ability of T-47D and MCF7 cells. **P<0.001 vs. si-NC or inhibitor-NC; $^{\#\#}$P<0.001 vs. inhibitor + si-CDK1 using two-way ANOVA. miR, microRNA; CDK1, cyclin-dependent kinase 1; si, small interfering; NC, negative control.

Discussion

The present study investigated the function and molecular mechanism of miR-337-3p in BC. The results demonstrated that miR-337-3p plays a key role in BC by targeting CDK1. miR-337-3p decreased the mRNA and protein expression levels of CDK1 in BC cells. In addition, miR-337-3p suppressed the progression of BC by modulating cellular processes, such as cell proliferation, adhesion, migration, invasion and cell apoptosis by targeting CDK1.

miR-337-3p has been extensively studied as a tumor suppressor in different types of cancer, such as hepatocellular carcinoma, non-small cell lung cancer, cervical cancer and clear cell renal cell carcinoma (ccRCC) (6-8,24,25). miR-337-3p has been reported to be expressed at low levels in ccRCC cells, and overexpression of miR-337-3p decreases cell proliferation and invasion in ccRCC and hepatocellular carcinoma (6,7). A previous study demonstrated that high miR-337-3p expression is associated with a higher 5-year survival rate in patients with HCC (7). In BC, Du *et al* (9) demonstrated that miR-337-3p targets STAT3, thereby inhibiting EMT in BC with chronic stress (9). The results of the present study were consistent with previous findings (6,8). miR-337-3p was aberrantly expressed at low levels in BC cells, and miR-337-3p overexpression inhibited the proliferation, adhesion, migration and invasion of BC cells, but activated cell apoptosis. However, in contrast to the study by Du *et al* (9), the results of the present study demonstrated that CDK1 was the downstream target of miR-337-3p and relieved the inhibitory effect of miR-337-3p on BC cells. Taken together, these results suggest that miR-337-3p may target multiple genes to play an antitumor role in BC.

Numerous studies have confirmed that CDK1 plays an oncogenic role in different types of cancer, including melanoma (26), gastric cancer (27) and bladder cancer (14). For example, CDK1 activates tumorigenesis in melanoma (26). High cytoplasmic CDK1 expression is a key predictor of poor overall survival in patients with epithelial ovarian cancer (15). Furthermore, CDK1 has been demonstrated to activate the proliferation of BC cells, and functions as an effective target in BC therapy (16). In the present study, functional assays demonstrated that inhibition of CDK1 decreased cell proliferation, adhesion, migration and invasion, but increased cell apoptosis in BC, which is consistent with a previous study (16). To the best of our knowledge, the present study was the first to demonstrate that miR-337-3p targets CDK1 in BC cells, thereby regulating the positive effect of CDK1 on BC cells. A previous study suggested that CDK1 associated with cyclin B is the primary stimulus for the entry of cells into mitosis (28); therefore, the miR-337-3p/CDK1 axis may regulate the cell cycle and play a key role in regulating the malignancy of BC cells.

The present study only investigated the function and regulation of the miR-337-3p/CDK1 axis at the cellular level

in vitro; however, animal experiments are essential for further characterization of its *in vivo* functions. The process of BC tumorigenesis and progression is complex. The present study confirmed the interaction between miR-337-3p and CDK1; however, further studies are required to determine other downstream mechanisms in BC.

In conclusion, the results of the present study demonstrated that miR-337-3p was expressed at low levels in BC tissues and cells, and plays a tumor suppressive role in the progression of BC cells by targeting CDK1. CDK1 activates BC cell progression and miR-337-3p modulates BC progression by decreasing the mRNA and protein expression levels of CDK1 in BC cells. Taken together, these results provide insight and potential targets for the design of effective therapies for the treatment of BC.

Acknowledgements

Not applicable.

Funding

No funding was received.

Availability of data and materials

The datasets used and/or analyzed during the current study are available from the corresponding author upon reasonable request.

Authors' contributions

SXK and JYL performed the experiments and analyzed the data. BZ and FL conceived and designed the present study. YY and TQ acquired the data, and confirmed the authenticity of all the raw data. YY, TQ and SXK analyzed and interpreted the data. All authors have read and approved the final manuscript.

Ethics approval and consent to participate

The present study was approved by the Ethics Committee of the People's Hospital of Zhengzhou University (Zhengzhou, China; approval no. 2019-10), and performed in accordance with the Declaration of Helsinki. Written informed consent was provided by all patients prior to the study start.

Patient consent for publication

Not applicable.

Competing interests

The authors declare that they have no competing interests.

References

1. Li T, Mello-Thoms C and Brennan PC: Descriptive epidemiology of breast cancer in China: Incidence, mortality, survival and prevalence. Breast Cancer Res Treat 159: 395-406, 2016.
2. DeSantis CE, Ma J, Gaudet MM, Newman LA, Miller KD, Sauer AG, Jemal A and Siegel RL: Breast cancer statistics, 2019. CA Cancer J Clin 69: 438-451, 2019.
3. Wei YT, Guo DW, Hou XZ and Jiang DQ: miRNA-223 suppresses FOXO1 and functions as a potential tumor marker in breast cancer. Cell Mol Biol (Noisy-le-grand) 63: 113-118, 2017.
4. Li P, Xu T, Zhou X, Liao L, Pang G, Luo W, Han L, Zhang J, Luo X, Xie X and Zhu K: Downregulation of miRNA-141 in breast cancer cells is associated with cell migration and invasion: Involvement of ANP32E targeting. Cancer Med 6: 662-672, 2017.
5. Bertoli G, Cava C and Castiglioni I: MicroRNAs: New biomarkers for diagnosis, prognosis, therapy prediction and therapeutic tools for breast cancer. Theranostics 5: 1122-1143, 2015.
6. Zhuang Q, Shen J, Chen Z, Zhang M, Fan M, Xue D, Lu H, Xu R, He X and Hou J: miR-337-3p suppresses the proliferation and metastasis of clear cell renal cell carcinoma cells via modulating Capn4. Cancer Biomark 23: 515-525, 2018.
7. Zuo XL, Chen ZQ, Wang JF, Wang JG, Liang LH and Cai J: miR-337-3p suppresses the proliferation and invasion of hepatocellular carcinoma cells through targeting JAK2. Am J Cancer Res 8: 662-674, 2018.
8. Cao XM: Role of miR-337-3p and its target Rap1A in modulating proliferation, invasion, migration and apoptosis of cervical cancer cells. Cancer Biomark 24: 257-267, 2019.
9. Du P, Zeng H, Xiao Y, Zhao Y, Zheng B, Deng Y, Liu J, Huang B, Zhang X and Yang K: Chronic stress promotes EMT-mediated metastasis through activation of STAT3 signaling pathway by miR-337-3p in breast cancer. Cell Death Dis 11: 761, 2020.
10. Zhou Y, Shen JK, Hornicek FJ, Kan Q and Duan Z: The emerging roles and therapeutic potential of cyclin-dependent kinase 11 (CDK11) in human cancer. Oncotarget 7: 40846-40859, 2016.
11. Tong W, Han TC, Wang W and Zhao J: LncRNA CASC11 promotes the development of lung cancer through targeting microRNA-302/CDK1 axis. Eur Rev Med Pharmacol Sci 23: 6539-6547, 2019.
12. Piao J, Zhu L, Sun J, Li N, Dong B, Yang Y and Chen L: High expression of CDK1 and BUB1 predicts poor prognosis of pancreatic ductal adenocarcinoma. Gene 701: 15-22, 2019.
13. Sung WW, Lin YM, Wu PR, Yen HH, Lai HW, Su TC, Huang RH, Wen CK, Chen CY, Chen CJ and Yeh KT: High nuclear/cytoplasmic ratio of Cdk1 expression predicts poor prognosis in colorectal cancer patients. BMC Cancer 14: 951, 2014.
14. Tian Z, Cao S, Li C, Xu M, Wei H, Yang H, Sun Q, Ren Q and Zhang L: LncRNA PVT1 regulates growth, migration, and invasion of bladder cancer by miR-31/ CDK1. J Cell Physiol 234: 4799-4811, 2019.
15. Yang W, Cho H, Shin HY, Chung JY, Kang ES, Lee EJ and Kim JH: Accumulation of cytoplasmic Cdk1 is associated with cancer growth and survival rate in epithelial ovarian cancer. Oncotarget 7: 49481-49497, 2016.
16. Izadi S, Nikkhoo A, Hojjat-Farsangi M, Namdar A, Azizi G, Mohammadi H, Yousefi M and Jadidi-Niaragh F: CDK1 in breast cancer: Implications for theranostic potential. Anticancer Agents Med Chem 20: 758-767, 2020.
17. Wilhite SE and Barrett T: Strategies to explore functional genomics data sets in NCBI's GEO database. Methods Mol Biol 802: 41-53, 2012.
18. Szklarczyk D, Gable AL, Lyon D, Junge A, Wyder S, Huerta-Cepas J, Simonovic M, Doncheva NT, Morris JH, Bork P, *et al*: STRING v11: Protein-protein association networks with increased coverage, supporting functional discovery in genome-wide experimental datasets. Nucleic Acids Res 47: D607-D613, 2019.
19. Liu J, Lichtenberg T, Hoadley KA, Poisson LM, Lazar AJ, Cherniack AD, Kovatich AJ, Benz CC, Levine DA, Lee AV, *et al*: An integrated TCGA pan-cancer clinical data resource to drive high-quality survival outcome analytics. Cell 173: 400-416.e411, 2018.
20. Nagy Á, Munkácsy G and Győrffy B: Pancancer survival analysis of cancer hallmark genes. Sci Rep 11: 6047, 2021.
21. Wu B, Liu G, Jin Y, Yang T, Zhang D, Ding L, Zhou F, Pan Y and Wei Y: miR-15b-5p promotes growth and metastasis in breast cancer by targeting HPSE2. Front Oncol 10: 108, 2020.
22. Agarwal V, Bell GW, Nam JW and Bartel DP: Predicting effective microRNA target sites in mammalian mRNAs. ELife 12: e05005, 2015.
23. Livak KJ and Schmittgen TD: Analysis of relative gene expression data using real-time quantitative PCR and the 2(-Delta Delta C(T)) method. Methods 25: 402-408, 2001.
24. Tang D, Zhao L, Peng C, Ran K, Mu R and Ao Y: LncRNA CRNDE promotes hepatocellular carcinoma progression by upregulating SIX1 through modulating miR-337-3p. J Cell Biochem 120: 16128-16142, 2019.

25. Li Q, Huang Q, Cheng S, Wu S, Sang H and Hou J: Circ_ZNF124 promotes non-small cell lung cancer progression by abolishing miR-337-3p mediated downregulation of JAK2/STAT3 signaling pathway. Cancer Cell Int 19: 291, 2019.
26. Menon DR, Luo Y, Arcaroli JJ, Liu S, KrishnanKutty LN, Osborne DG, Li Y, Samson JM, Bagby S, Tan AC, *et al*: CDK1 Interacts with Sox2 and promotes tumor initiation in human melanoma. Cancer Res 78: 6561-6574, 2018.
27. Zhang L, Kang W, Lu X, Ma S, Dong L and Zou B: LncRNA CASC11 promoted gastric cancer cell proliferation, migration and invasion in vitro by regulating cell cycle pathway. Cell Cycle 17: 1886-1900, 2018.
28. Xie D, Song H, Wu T, Li D, Hua K, Xu H, Zhao B, Wu C, Hu J, Ji C, *et al*: MicroRNA-424 serves an anti-oncogenic role by targeting cyclin-dependent kinase 1 in breast cancer cells. Oncol Rep 40: 3416-3426, 2018.